Available online at www.sciencedirect.com
ScienceDirect
Journal of Power Sources 166 (2007) 211–218
JOURNAL OF POWER SOURCES
www.elsevier.com/locate/jpowsour

Effect of mechanical activation process parameters on the properties of $LiFePO_4$ cathode material

Jae-Kwang Kim [a], Gouri Cheruvally [a], Jae-Won Choi [a], Jong-Uk Kim [a], Jou-Hyeon Ahn [a,*], Gyu-Bong Cho [b], Ki-Won Kim [b], Hyo-Jun Ahn [b]

[a] *Department of Chemical and Biological Engineering, ITRC for Energy Storage and Conversion, Gyeongsang National University, 900 Gajwa-dong, Jinju 660-701, Republic of Korea*
[b] *Division of Advanced Materials Science and Engineering, ITRC for Energy Storage and Conversion, Gyeongsang National University, 900 Gajwa-dong, Jinju 660-701, Republic of Korea*

Received 19 October 2006; accepted 29 December 2006
Available online 18 January 2007

Abstract

Pure, nano-sized $LiFePO_4$ and carbon-coated $LiFePO_4$ ($LiFePO_4$/C) positive electrode (cathode) materials are synthesized by a mechanical activation process that consists of high-energy ball milling and firing steps. The influence of the processing parameters such as firing temperature, firing time and ball-milling time on the structure, particle size, morphology and electrochemical performance of the active material is investigated. An increase in firing temperature causes a pronounced growth in particle size, especially above 600 °C. A firing time longer than 10 h at 600 °C results in particle agglomeration; whereas, a ball milling time longer than 15 h does not further reduce the particle size. The electrochemical properties also vary considerably depending on these parameters and the highest initial discharge capacity is obtained with a $LiFePO_4$/C sample prepared by ball milling for 15 h and firing for 10 h at 600 °C. Comparison of the cyclic voltammograms of $LiFePO_4$ and $LiFePO_4$/C shows enhanced reaction kinetics and reversibility for the carbon-coated sample. Good cycle performance is exhibited by $LiFePO_4$/C in lithium batteries cycled at room temperature. At the high current density of 2*C*, an initial discharge capacity of 125 mAh g^{-1} (73.5% of theoretical capacity) is obtained with a low capacity fading of 0.18% per cycle over 55 cycles.

Keywords: $LiFePO_4$; Mechanical activation; Rechargeable lithium battery; Discharge capacity; Cathode material; Cycling performance

1. Introduction

$LiCoO_2$, which is currently used as the positive electrode (cathode) material in commercial lithium batteries, needs to be replaced for better performance, lower cost and increased safety, especially for applications in large batteries for back-up power systems, electric and hybrid electric vehicles, and load-leveling systems [1]. Consequently, olivine-type $LiFePO_4$ has attracted much attention as a new cathode active material with these desired features. Since the first report of reversible lithium insertion/extraction with $LiFePO_4$ by Padhi et al. [2], significant research has focused on developing it into a commercially acceptable cathode material [3,4]. $LiFePO_4$ offers several advantages namely: (i) a relatively high theoretical specific capacity of 170 mAh g^{-1}; (ii) a perfectly flat discharge voltage at 3.4 V *versus* lithium, which provides for a wider safety margin of usage for organic electrolytes; (iii) good reversibility of cathode reactions; (iv) high thermal and chemical stability; (v) low material cost; (vi) low toxicity; (vii) improved safety. The olivine structure is quite stable and mechanically robust. On lithium extraction, $LiFePO_4$ changes to $FePO_4$, which has a strikingly similar structure with a volume change of only 6.81% [2]. These factors lead to good performance of cells on repeated cycling. In spite of these attractive features, $LiFePO_4$ requires further modifications to overcome limitations of poor electronic conductivity ($\sim 10^{-9}$ S cm^{-1}) [5] and slow lithium ion diffusion [6]. Conductivity is enhanced appreciably by coating $LiFePO_4$ particles with conductive materials such as carbon [7–15], or metal [16], dispersing metal particles [17], and solid-solution doping by cations [8,18,19]. Synthesizing small particles (with lower dif-

* Corresponding author. Tel.: +82 55 751 5388; fax: +82 55 753 1806.
E-mail address: jhahn@gsnu.ac.kr (J.-H. Ahn).

0378-7753/$ – see front matter © 2007 Elsevier B.V. All rights reserved.
doi:10.1016/j.jpowsour.2006.12.089

fusion length) of phase-pure material with high specific surface area has been investigated as a means to enhance ion diffusion [20].

The electrochemical performance of a cathode based on $LiFePO_4$ or carbon-coated $LiFePO_4$ ($LiFePO_4$/C) depends on a number of factors, e.g., phase purity, particle size, morphology, amount of carbon, and effectiveness of carbon contact. Since most of these factors are dependent on the synthesis route, adopting the most suitable method and controlling the processing conditions are crucial in realizing a material with high performance. $LiFePO_4$ has been synthesized by different methods including solid-state reaction [20–23], mechanical activation (MA) [13–15,24,25], microwave heating [26], sol–gel [27–31], and aqueous/non-aqueous precipitation [32–34]. The crystalline olivine phase of $LiFePO_4$ is generally formed from the amorphous precursor by thermal treatment at high temperature, most often >500 °C. The synthesis of extremely pure $LiFePO_4$ is difficult because of the +2 oxidation state of iron in the compound. The conversion of ferrous to ferric is usually avoided by conducting the reactions in an inert gas atmosphere. The solid-state route is widely adopted for synthesis because it generally results in phase-pure $LiFePO_4$. Nevertheless, repeated steps of calcination, grinding and heating for long duration at high temperatures are needed to obtain a single-phase olivine product [20,21]. Recent studies have shown that MA is a promising method for synthesis of $LiFePO_4$ [13–15,24,25], in which the reactants are subjected to an initial thorough mixing in a high-energy ball mill that results in pulverization and intimate powder mixing. It has been found that a ball-milling step alone is insufficient to obtain a single-phase olivine product. On the other hand, the time and temperature of the thermal treatment necessary for final crystallization of the compound can be decreased substantially by this process [13,15].

This study examines the influence of process parameters on the properties of $LiFePO_4$ and $LiFePO_4$/C (using carbon black as the conductive coating) active materials synthesized by the MA process. The effects of ball milling and thermal processing conditions on the phase-purity, particle size, morphology and electrochemical performance of the materials are investigated. The cycle performance of lithium cells with these active materials as cathodes is also evaluated.

2. Experimental

2.1. Synthesis

$LiFePO_4$ was synthesized from Li_2CO_3, $FeC_2O_4{\cdot}2H_2O$ and $NH_4H_2PO_4$ (all chemicals of 99% purity from Aldrich) taken in stoichiometric quantities. The MA process consisted of the following steps: (i) high-energy ball milling of the powder in a hardened steel vial with zirconia balls (ball-to-powder weight ratio = 10:3) at room temperature for different periods in an argon atmosphere using a SPEX mill at 1000 rpm; (ii) conversion of the powder into pellets by mechanical pressing; (iii) thermal treatment of the pellets at temperatures ranging from 500 to 700 °C for different time intervals in a nitrogen atmosphere; (iv) slow cooling to room temperature. For preparing $LiFePO_4$/C, a mixture of the above raw materials and 7.8 wt.% of acetylene black powder (Alfa, purity >99.9%) was used; the processing steps remained the same.

2.2. Characterization

The crystallographic structures of the synthesized materials were analyzed by X-ray powder diffraction (XRD: D8 Advance, Bruker AXS) using Cu Kα radiation. The crystallite size was calculated by the Scherrer equation, $\sigma = \lambda/(\beta_{2\theta}\cos\theta)$, from the integral width β of five strong, well-resolved reflection peaks corresponding to the [2 0 0], [1 0 1], [0 1 1], [1 1 1] and [2 1 1] crystallographic directions and the mean value was calculated [27,32]. The morphology was studied by means of scanning electron microscopy (SEM: JEOL JSM 5600) and the nature of carbon coating was examined using transmission electron microscopy (TEM: JEM-2010, JEOL). The specific surface-area of the samples, S_s, was measured by means of the Brunauer, Emmett, Teller (BET) method (ASAP 2010 Analyzer). The estimated equivalent spherical diameter R_{BET} (nm) was calculated from S_s ($m^2\,g^{-1}$) data and sample density ρ_t ($g\,cm^{-3}$) using the relation, $R_{BET} = 6000/(\rho_t S_s)$ [33].

2.3. Electrochemical evaluation

To prepare the cathode, the active material powder, carbon black and poly(vinylidene fluoride) (PVdF: Aldrich) binder were mixed in the ratio 60:20:20 by weight. A viscous slurry in NMP solvent was cast on aluminum foil and dried at 95 °C under vacuum for 12 h. The film was cut into circular discs of area 0.95 cm^2 and mass ~3.0 mg for use as cathodes. Two-electrode electrochemical coin cells were assembled with a lithium-metal anode, a Celgard®-2200 separator, a 1 M $LiPF_6$ in EC:DMC (1:1 vol%) electrolyte, and a $LiFePO_4$/C (or $LiFePO_4$) cathode. Cyclic voltammetry was performed at a scan rate of 0.1 mV s^{-1} between 2.0 and 4.5 V. Electrochemical performance tests were conducted in an automatic galvanostatic charge–discharge unit, WBCS3000 battery cycler, between 2.0 and 4.6 V at room temperature. The experiments were undertaken at different current density rates that ranged from C/30 to 2C.

3. Results and discussion

In a comparison of different synthesis routes for $LiFePO_4$ such as solid-state reaction, co-precipitation in aqueous medium, hydrothermal and MA methods, Franger et al. [25] found that the MA process is superior to the others in achieving the optimum material with good electrochemical performance. Fine particles of $LiFePO_4$/C, prepared by the MA process, with enhanced properties have been reported by other researchers [11,13–15]. Here we present the results of a parametric study of the influence of different MA processing parameters on the properties of $LiFePO_4$ and $LiFePO_4$/C.

The effect of firing temperature on the XRD spectra of $LiFePO_4$ and $LiFePO_4$/C is shown in Fig. 1. The samples were prepared by ball milling for 4 h and heating for 10 h at different temperatures of 500, 600 and 700 °C. The diffraction patterns

Table 1
Properties of $LiFePO_4$ and $LiFePO_4$/C prepared at different temperatures (ball milling for 4 h and thermal treatment for 10 h)

Properties	$LiFePO_4$ prepared at			$LiFePO_4$/C prepared at		
	500 °C	600 °C	700 °C	500 °C	600 °C	700 °C
Average crystal size[a] (nm)	38	43	52	29	33	40
Particle size range[b] (nm)	75–123	80–148	315–775	50–95	60–115	200–395
Average particle size[b] (nm)	95	105	491	67	80	298

[a] Estimated from XRD data.
[b] Estimated from SEM data.

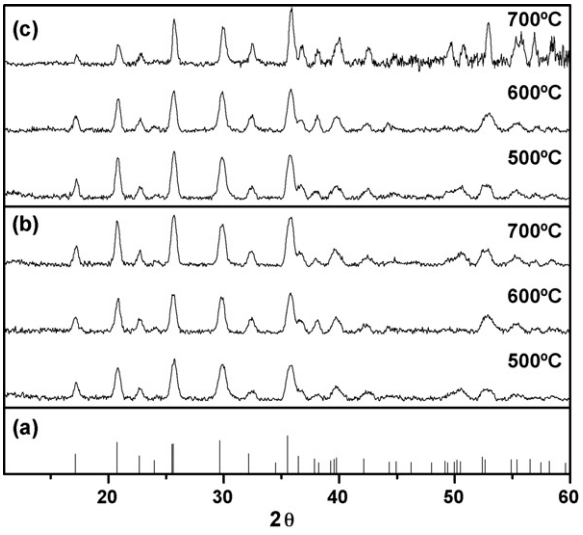

Fig. 1. XRD spectra of (a) standard *Pnma* orthorhombic $LiFePO_4$, (b) $LiFePO_4$ and (c) $LiFePO_4$/C samples, prepared at different temperatures of 500, 600 and 700 °C (4 h ball milling and 10 h heating).

remain the same for all the samples and the structure is identified to belong to the orthorhombic *Pnma* space group. The characteristic peaks of $LiFePO_4$ are formed even at the lowest temperature of 500 °C. The crystallization temperature of $LiFePO_4$ has been reported to be ~567 °C, based on a differential thermal analysis study [33]. By contrast, from differential scanning calorimetry studies, Franger et al. [25] have reported a decrease in the crystallization temperature of $LiFePO_4$ from 502 to 432 °C if the reactants are intimately mixed by the MA process. In the present study, it is inferred that considerable crystallization of mechanically activated ingredients has occurred under firing at 500 °C. Nevertheless, the crystalline peak intensities of the 500 °C samples are less than those of samples prepared at higher temperatures. Parasitic peaks or impurities are not detected in the XRD spectra. The average crystal size was calculated based on the spectra and given in Table 1. It is found that the crystal size increases with firing temperature, as observed in earlier studies [32]. The crystal size of the $LiFePO_4$/C sample is smaller than that of the corresponding $LiFePO_4$ sample, which conforms that carbon inhibits the particle growth to a considerable extent [22].

The effect of firing temperature on the particle size and morphology was studied by SEM. The micrographs obtained for $LiFePO_4$ and $LiFePO_4$/C prepared by ball milling for 4 h and heating for 10 h at different temperatures are shown in Fig. 2. Near-spherical, nano-meter sized particles with minimal agglomeration are obtained for both $LiFePO_4$ and $LiFePO_4$/C. The average particle size (estimated from SEM analysis, given in Table 1) does not vary much for samples prepared at 500 and 600 °C, but increases substantially for samples prepared at 700 °C. It is likely that the firing condition at 500 °C is insufficient for complete crystallization of $LiFePO_4$ (as is also observed in XRD analysis) and the small particles become slightly agglomerated. At 600 °C, crystallization is apparently

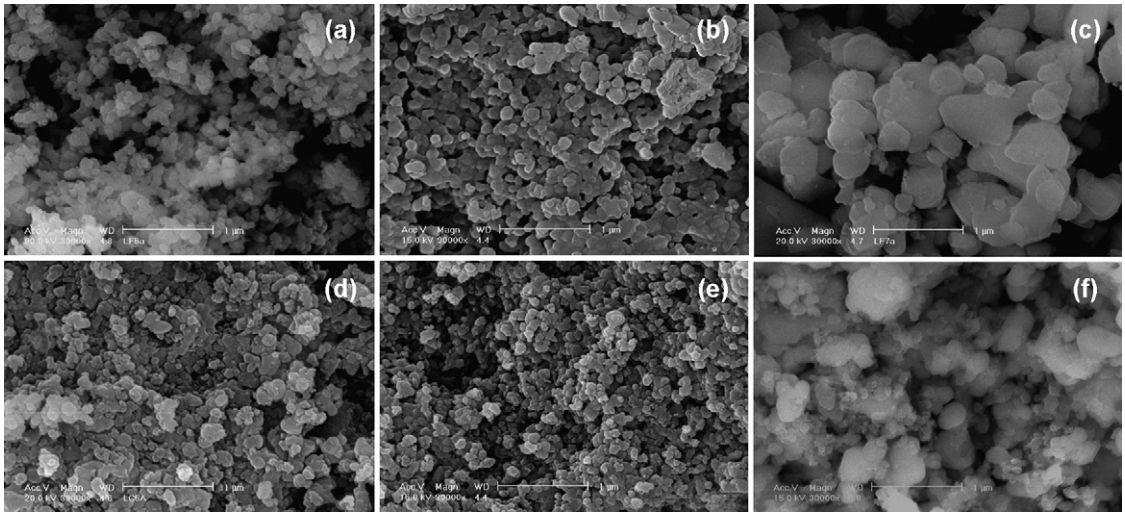

Fig. 2. Scanning electron micrographs of samples prepared at different temperatures: (a)–(c) $LiFePO_4$ at 500, 600 and 700 °C, respectively; (d)–(f) $LiFePO_4$/C at 500, 600 and 700 °C, respectively (ball milling for 4 h and thermal treatment for 10 h).

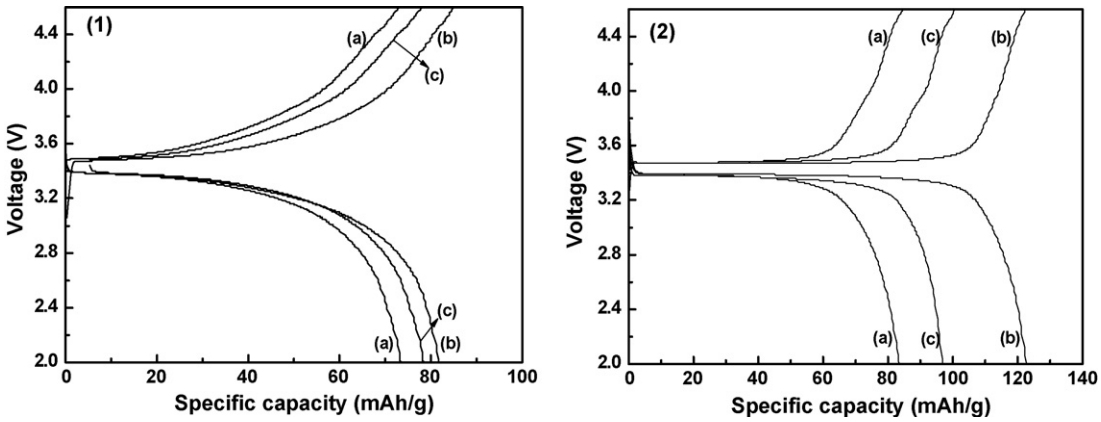

Fig. 3. Initial charge and discharge capacities of samples prepared at different temperatures (a) 500, (b) 600 and (c) 700 °C: (1) $LiFePO_4$, and (2) $LiFePO_4$/C (ball milling for 4 h and thermal treatment for 10 h).

completed and the particles attain a more compact structure without any substantial increase in size, compared with the 500 °C sample. Undesirable particle growth occurs at 700 °C and leads to larger particles that are nearly 4–5 times the size of those formed at 600 °C. A similar increase in particle size at higher firing temperatures has been observed by other workers [13,23,33]. Compared with $LiFePO_4$, $LiFePO_4$/C particles are smaller in size due to the inhibition of crystal growth to a great extent by the presence of carbon in the reaction mixture [13,22]. Generally, an increase in firing temperature increases the surface smoothness [13], and compared with $LiFePO_4$, the carbon coating in $LiFePO_4$/C provides a comparatively rougher surface texture for the particles. The specific surface-area determined for the $LiFePO_4$/C samples prepared at 500, 600 and 700 °C is 15.0, 15.6 and 6.4 $m^2\ g^{-1}$, respectively. The equivalent spherical diameters are 119, 114 and 280 nm, respectively; these values agree with the particle size range estimated from SEM studies.

The electrochemical performance in terms of the initial charge–discharge capacities of $LiFePO_4$ and $LiFePO_4$/C prepared at different firing temperatures are compared in Fig. 3(1) and (2), respectively. The characteristic flat discharge plateau at ~3.4 V, which represents a two-phase reaction in the electrode, is observed for all the samples. Thus, the electrode is affected neither by the preparation temperature nor by the presence of carbon coating [23]. The difference between the charging and discharging voltages is lower for $LiFePO_4$/C (0.08 V) than for $LiFePO_4$ (0.22 V); the conductive carbon coating is seen to improve the kinetics of the redox reaction occurring at the solid interface. The discharge capacities for $LiFePO_4$ prepared at 500, 600 and 700 °C are 74, 82 and 79 mAh g^{-1}, respectively, and 84, 123 and 97 mAh g^{-1} for the corresponding $LiFePO_4$/C samples. The inferior performance of $LiFePO_4$ is attributed to its inherently low electronic and low ionic conductivity [5,6] and firing temperature variation results in only <10% change in its discharge capacity. By contrast, the firing temperature substantially influences the discharge performance of $LiFePO_4$/C with an increase of 46% for the sample prepared at 600 °C compared with that at 500 °C. $LiFePO_4$/C with conductive carbon coating exhibits higher performance compared with uncoated counterparts. The sample prepared at 600 °C, which has small particles with uniform morphology, is found to be the optimum. The 500 °C sample performed least, although it had a particle size comparable with that of the 600 °C sample. The lower utilization of the 500 °C sample could be due to its lower level of crystallinity. The larger particles of the 700 °C sample result in a lower performance than the 600 °C sample with the optimum particle size and purity level.

Further studies have been undertaken with $LiFePO_4$/C prepared at the optimum temperature of 600 °C. The effect of firing time on the morphology is presented in Fig. 4. The samples were ball milled for 4 h, followed by thermal treatment at 600 °C for different time intervals of 5, 10 and 24 h. The average particle sizes for these samples estimated from SEM are 187, 80 and 165 nm, respectively. The most uniform morphology with the least agglomeration and a homogenous dispersion of particles is obtained for the sample with a heating time of 10 h. The initial discharge capacities of these samples are compared in Fig. 5. As expected from SEM results, the sample heated for 10 h with

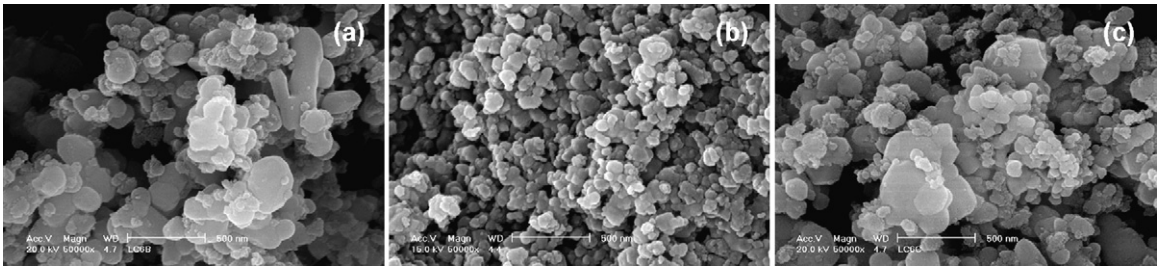

Fig. 4. Scanning electron micrographs of $LiFePO_4$/C samples prepared under different heating time at 600 °C: (a) 5 h, (b) 10 h, and (c) 24 h (ball milling: 4 h).

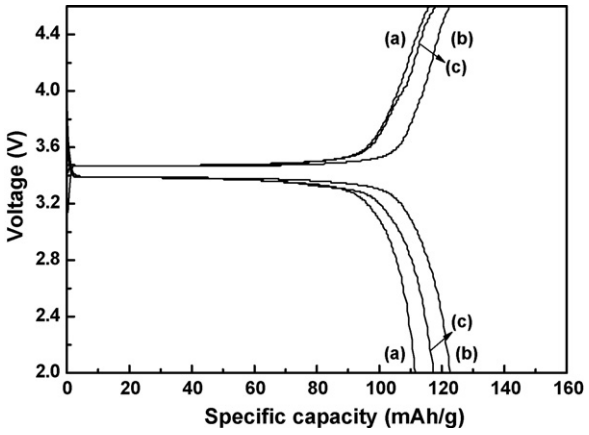

Fig. 5. Initial charge and discharge capacities of $LiFePO_4$/C samples prepared under different heating time at 600 °C: (a) 5 h, (b) 10 h, and (c) 24 h (ball milling: 4 h).

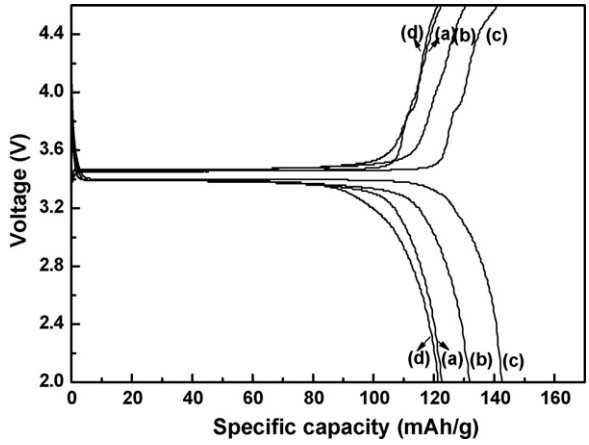

Fig. 7. Initial charge and discharge capacities of $LiFePO_4$/C samples prepared under different ball milling times: (a) 4 h, (b) 10 h, (c) 15 h, and (d) 24 h (thermal treatment at 600 °C, 10 h).

the smallest particle size and uniform morphology exhibited the highest discharge capacity, followed by the 24 h sample. Thermal treatment for 5 h appears to be insufficient in generating a fully crystalline phase of the particles and results in larger particle with lower performance.

The effect of ball milling time on the morphology and discharge capacity of $LiFePO_4$/C samples prepared by thermal treatment at 600 °C for 10 h are shown in Figs. 6 and 7, respectively. The average particle sizes of the samples prepared with ball milling time of 4, 10, 15 and 24 h are 80, 77, 72 and 72 nm, respectively. The particle size reduces slightly with higher milling time and there is little effect after 15 h. At the same time, the tendency for agglomeration is enhanced after 15 h, as seen in SEM images. The optimum electrochemical performance is shown by the sample ball milled for 15 h. A very short milling time, e.g., 4 h, seems insufficient for a homogenous grinding of all the solid materials uniformly.

The results obtained in this parametric study testify that the processing parameters of the MA method employed for the synthesis of $LiFePO_4$/C have a profound influence on the physical properties of the material that, in turn, dictate the electrochemical performance. The initial discharge capacity at room temperature is found to vary by 46% maximum over the temperature range 500–700 °C, by <10% over the heating time 5–24 h at 600 °C, and by ∼18% over a ball milling time of 4–24 h and subsequent firing for 10 h at 600 °C. Phase-pure $LiFePO_4$/C with small particle size, uniform morphology and least agglomeration performs best in electrochemical tests. The optimum processing

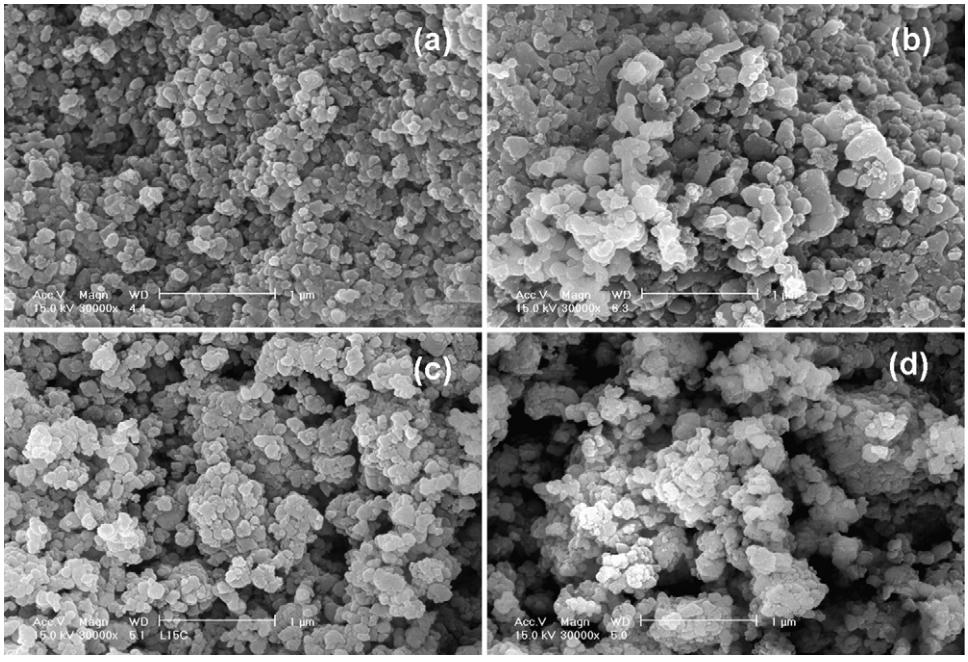

Fig. 6. Scanning electron micrographs of $LiFePO_4$/C samples prepared under different ball milling times: (a) 4 h, (b) 10 h, (c) 15 h, and (d) 24 h (thermal treatment at 600 °C, 10 h).

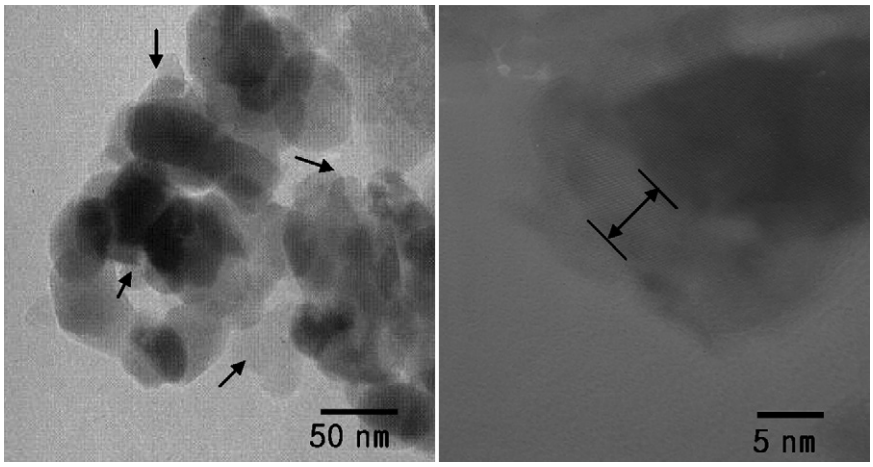

Fig. 8. Transmission electron micrograph of $LiFePO_4$/C prepared at 600 °C: arrow indicates carbon coating.

conditions based on the initial discharge capacity evaluation are found to be 15 h ball milling followed by 10 h firing at 600 °C. The remaining part of the study reported here was undertaken with materials prepared under these optimum conditions.

For carbon-coated $LiFePO_4$, the nature and uniformity of the carbon coating are important factors that decide the electrochemical properties [7,8,10]. The carbon coating obtained for the sample prepared in this study was analyzed by TEM and is shown in Fig. 8. An amorphous carbon coating with a thickness in the range of 4–10 nm and an average thickness of 6 nm is observed. The coating appears to be thin and porous and surrounds all the $LiFePO_4$ particles. Knowing the specific surface-area of the particles (15.6 $m^2\,g^{-1}$), carbon content (13.96 wt.%), and the true density of carbon (1.8–2.1 $g\,cm^{-3}$), the approximate thickness of the carbon coating is theoretically calculated to be ∼5 nm. Thus, it is seen that the MA process with carbon incorporated along with other ingredients initially can result in active particles with a uniform and thin coating of the conductive matrix.

The results of CV experiments on $LiFePO_4$ and $LiFePO_4$/C are presented in Fig. 9(a) and (b), respectively. Anodic and cathodic peaks appear at ∼3.6 and ∼3.3 V, respectively, with the mean redox potential at 3.4 V, for both materials. The area under the anodic and cathodic peaks remains nearly the same and thus shows that an equal quantity of lithium ions can be reversibly extracted and inserted into the materials. The main differences between $LiFePO_4$ and $LiFePO_4$/C are in the redox current, shouldering of the voltammogram, and the change in curve with cycle number. The redox current for $LiFePO_4$/C (0.62 mA) is more than double that for $LiFePO_4$ (0.26 mA). The smaller redox current for uncoated particles results from its lower utilization because of its poor electronic conductivity and limited lithium ion diffusivity due to larger particle size, compared with the carbon-coated particles. These kinetic limitations also lead to the shouldering of CV curves. The improved electron and ion diffusion possibilities in the coated $LiFePO_4$/C may result in better reversibility of the redox reactions over repeated cycling as well. The enhancement of the charge-transfer kinetics of $LiFePO_4$ with a carbon coating has been reported earlier based on CV measurements [15] as well as impedance spectroscopy measurements [35].

The cycle performance of lithium cells using $LiFePO_4$/C as the cathode was evaluated up to 55 cycles at different current densities and the results are presented in Fig. 10. The initial discharge capacities obtained at *C*/30, *C*/10, 1*C* and 2*C* rates are 148, 143, 134 and 125 mAh g^{-1}, respectively. A decrease in initial discharge capacity with current density results from

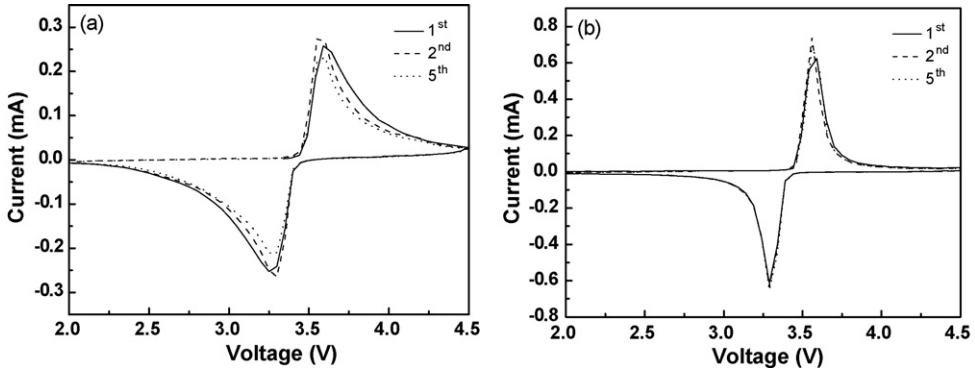

Fig. 9. Cyclic voltammograms at room temperature of Li cells with cathodes: (a) $LiFePO_4$, and (b) $LiFePO_4$/C. Scan rate: 0.1 mV s^{-1}, voltage range: 2.0–4.5 V.

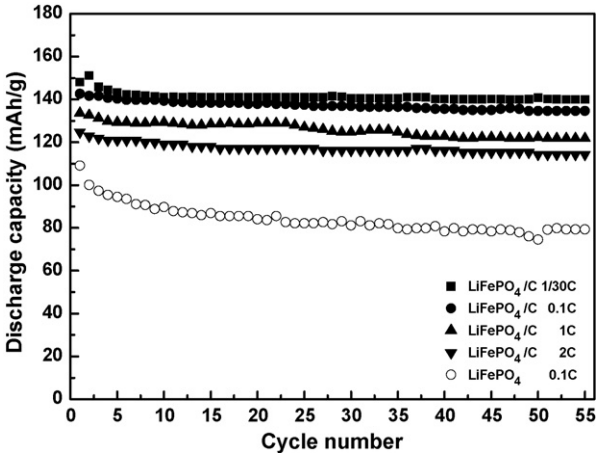

Fig. 10. Cycle performance of lithium cells at room temperature with $LiFePO_4$ and $LiFePO_4$/C cathodes at different current densities.

the intrinsic lithium ion diffusion limitations of the material [6]. Nevertheless, a good cycling property is shown even at the high current density of 2*C* at room temperature. After 55 cycles at 2*C*, a discharge capacity of 114 mAh g^{-1} is obtained (91% of its initial value) with only a low capacity fading of 0.18% per cycle. Although uncoated $LiFePO_4$ also provides a stable cycle performance, the capacity is inferior to that of $LiFePO_4$/C. Thus, after 55 cycles, $LiFePO_4$ has a discharge capacity of 79 mAh g^{-1} at the 0.1*C* rate, compared with 140 mAh g^{-1} for $LiFePO_4$/C.

4. Conclusions

The effect of processing parameters such as firing temperature, firing time and ball-milling time on the structural, morphological and electrochemical properties of $LiFePO_4$ and $LiFePO_4$/C synthesized by the MA process has been investigated. XRD analysis shows the formation of phase-pure materials, with an increase in crystal size at higher temperatures. SEM reveals a substantial increase in particle size with increase in firing temperature above 600 °C. Small and uniform particles with the least agglomeration are obtained by thermal treatment for 10 h at 600 °C. The initial discharge capacity at room temperature is found to vary by a maximum of 46% over the temperature range 500–700 °C, <10% over the heating time of 5–24 h at 600 °C, and ∼18% over the ball-milling time of 4–24 h and subsequent firing for 10 h at 600 °C. The optimum processing conditions based on the initial discharge capacity are found to be 15 h of ball-milling followed by 10 h of thermal treatment at 600 °C. $LiFePO_4$/C prepared under these optimized conditions exhibits initial discharge capacities of 148, 143, 134 and 125 mAh g^{-1} at *C*/30, *C*/10, 1*C* and 2*C* rates, respectively. A comparison of the CVs of uncoated and carbon-coated samples clearly shows the better reaction kinetics of the coated samples and the higher reversibility obtained in cycling for $LiFePO_4$/C. The cycle performance at different current densities reveals the good performance capability of $LiFePO_4$/C, with low capacity fading even at the high current density of 2*C*. $LiFePO_4$/C active material with good electrochemical performance can be realized by adopting the MA process for preparation under the optimized conditions.

Acknowledgements

This research was supported by the MIC (Ministry of Information and Communication), Korea, under the ITRC (Information Technology Research Center) support program supervised by the IITA (Institute of Information Technology Assessment). Gouri Cheruvally is grateful to the KOFST for the award of a Brain Pool Fellowship, and J.-K. Kim and J.-W. Choi acknowledge partial support by the Post Brain Korea 21 Project in 2006.

References

[1] K. Striebel, J. Shim, A. Sierra, H. Yang, X. Song, R. Kostecki, K. McCarthy, J. Power Sources 146 (2005) 33.
[2] A.K. Padhi, K.S. Nanjundaswamy, J.B. Goodenough, J. Electrochem. Soc. 144 (4) (1997) 1188.
[3] K. Zaghib, P. Charest, A. Guerfi, J. Shim, M. Perrier, K. Striebel, J. Power Sources 134 (2004) 124.
[4] K. Striebel, A. Guerfi, J. Shim, M. Armand, M. Gauthier, K. Zaghib, J. Power Sources 119–121 (2003) 951.
[5] S.Y. Chung, Y.M. Chiang, Electrochem. Solid State Lett. 6 (2003) A278.
[6] P.P. Prosini, M. Lisi, D. Zane, M. Pasquali, Solid State Ionics 148 (2002) 45.
[7] H. Huang, S.C. Yin, L.F. Nazar, Electrochem. Solid State Lett. 4 (2001) A170.
[8] T. Nakamura, Y. Miwa, M. Tabuchi, Y. Yamada, J. Electrochem. Soc. 153 (2006) A1108.
[9] R. Dominko, M. Bele, M. Gaberscek, M. Remskar, D. Hanzel, S. Pejovnik, J. Jamnik, J. Electrochem. Soc. 152 (2005) A607.
[10] M.M. Doeff, Y. Hu, F. McLarnon, R. Kostecki, Electrochem. Solid State Lett. 6 (2003) A207.
[11] Z. Chen, J.R. Dahn, J. Electrochem. Soc. 149 (2002) A1184.
[12] P.P. Prosini, D. Zane, M. Pasquali, Electrochim. Acta 46 (2001) 3517.
[13] S.J. Kwon, C.W. Kim, W.T. Jeong, K.S. Lee, J. Power Sources 137 (2004) 93.
[14] X.Z. Liao, Z.F. Ma, L. Wang, X.M. Zhang, Y. Jiang, Y.S. He, Eelctrochem. Solid State Lett. 7 (2004) A522.
[15] S. Franger, C. Bourbon, F.L. Cras, J. Electrochem. Soc. 151 (2004) A1024.
[16] K.S. Park, J.T. Son, H.T. Chung, S.J. Kim, C.H. Lee, K.T. Kang, H.G. Kim, Solid State Commun. 129 (2004) 311.
[17] F. Croce, A.D. Epifanio, J. Hassoun, A. Deptula, T. Olczac, B. Scrosati, Electrochem. Solid State Lett. 5 (2002) A47.
[18] J.F. Ni, H.H. Zhou, J.T. Chen, X.X. Zhang, Mater. Lett. 59 (2005) 2361.
[19] S. Shi, L. Liu, C. Ouyang, D.S. Wang, Z. Wang, L. Chen, X. Huang, Phys. Rev. B 68 (2003) 195108.
[20] A. Yamada, S.C. Chung, K. Hinokuma, J. Electrochem. Soc. 148 (2001) A224.
[21] H.S. Kim, B.W. Cho, W.I. Cho, J. Power Sources 132 (2004) 235.
[22] C.H. Mi, X.B. Zhao, G.S. Cao, J.P. Tu, J. Electrochem. Soc. 152 (2005) A483.
[23] M. Takahashi, S. Tobishima, K. Takei, Y. Sakurai, J. Power Sources 97–98 (2001) 508.
[24] N. Kosova, E. Devyatkina, Solid State Ionics 172 (2004) 181.
[25] S. Franger, F.L. Cras, C. Bourbon, H. Rouault, J. Power Sources 119–121 (2003) 252.
[26] K.S. Park, J.T. Son, H.T. Chung, S.J. Kim, C.H. Lee, H.G. Kim, Electrochem. Commun. 5 (2003) 839.
[27] M.A.E. Sanchez, G.E.S. Brito, M.C.A. Fantini, G.F. Goya, J.R. Matos, Solid State Ionics 177 (2006) 497.
[28] Y. Hu, M.M. Doeff, R. Kostecki, R. Finones, J. Electrochem. Soc. 151 (2004) A1279.

[29] J. Yang, J.J. Xu, J. Electrochem. Soc. 153 (4) (2006) A716.
[30] M. Piana, B.L. Cushing, J.B. Goodenough, N. Penazzi, Solid State Ionics 175 (2004) 233.
[31] J. Yang, J.J. Xu, Eelctrochem. Solid State Lett. 7 (2004) A515.
[32] G. Arnold, J. Garche, R. Hemmer, S. Strobele, C. Volger, M. Wohlfahrt-Mehrens, J. Power Sources 119–121 (2003) 247.
[33] S. Scaccia, M. Carewska, P. Wisniewski, P.P. Prosini, Mater. Res. Bull. 38 (2003) 1155.
[34] M.R. Yang, W.H. Ke, S.H. Wu, J. Power Sources 146 (2005) 539.
[35] S. Franger, F.L. Cras, C. Bourbon, H. Rouault, Electrochem. Solid State Lett. 5 (2002) A231.